

Anti-SARS-CoV-2 Activity of *Andrographis paniculata* (Burm.f.) Nees Extract via Inhibition of Spike-mediated Syncytia Formation in HEK293T Cell Model

Pekik Wiji Prasetyaningrum, Ria Fajarwati Kastian, Metta Novianti, Adi Santoso, Endah Puji Septisetyani*

Mammalian Cell Engineering Research Group, Research Center for Genetic Engineering, Research Organization for Life Sciences, The National Research and Innovation Agency of Republic Indonesia. Laboratory of Genomic, KST Soekarno, Cibinong, Bogor 16911, Indonesia

ARTICLE INFO

Article history:

Received March 20, 2024

Received in revised form May 13, 2024

Accepted May 20, 2024

KEYWORDS:

Andrographis paniculata (Burm.f.) Nees, antiviral, pseudovirus, Sambiloto, SARS-CoV-2, syncytia formation

ABSTRACT

The resurgence of COVID-19 endemic cases at the end of 2023 has underscored the need for effective treatments. Some severe cases of COVID-19 are often characterized by the formation of multinucleated syncytial pneumocytes in the lungs. Therefore, our study aimed to explore the potential of *Andrographis paniculata* (Burm. f) Nees as an antiviral against SARS-CoV-2, which involves syncytia formation. We utilized the non-toxic concentrations of *A. paniculata* extract on HEK293T cells determined by MTT assay, which were 1 µg/ml (cell viability 97.96%) and 10 µg/ml (cell viability 95.24%) for further assays. First, we conducted a pseudovirus cellular entry assay as a model of SARS-CoV-2 infection in HEK293T cells expressing hACE2/TMPRSS2. The HEK293T cells were co-transfected with plasmids expressing hACE2 and TMPRSS2, then infected with pseudotyped spike*ΔG-GFP rVSV with or without *A. paniculata* extract. The internalized pseudovirus would trigger GFP expression as a reporter of the infected cells. Next, we performed a syncytia assay by transfecting HEK293T cells with hACE2, TMPRSS2, and SARS-CoV-2 spike expression vectors to induce syncytia formation as a model of intercellular viral transmission. As the results, 10 µg/mL of the extract significantly lowered the number of SARS-CoV-2 pseudovirus-infected cells by 54.69% (P = 0.02) and spike-mediated syncytia formation by 42.39% (P<0.001). In conclusion, our results suggested that *A. paniculata* has a potential antiviral activity against SARS-CoV-2 by hindering virus infection and cell-to-cell transmission.

1. Introduction

By the end of 2023, the daily cases of SARS-CoV-2 infection numbers are globally increasing with new subvariants of SARS-CoV-2 omicron (EG.4 and EG.5), indicating the relentless COVID-19 pandemic, which currently shifted into an endemic era (Afifa 2023). In addition to vaccines, this phenomenon leads researchers to explore diverse avenues in the realm of medicinal plants. Among these medicinal plants, *Andrographis paniculata* (Burm.f) Nees (*A. paniculata*) has emerged as a promising candidate, with its primary bioactive compound, andrographolide, garnering increasing attention for its potential antiviral properties (Siridechakorn *et al.* 2023; Che *et*

al. 2023). As the world grapples with the challenge posed by the COVID-19 pandemic, the demand for innovative and accessible therapeutic options has never been more pronounced.

SARS-CoV-2 is categorized as a syncytial virus as well as another coronavirus such as SARS-CoV-1, MERS-CoV, and HKUI (Franks *et al.* 2003; Chan *et al.* 2013; Dominguez *et al.* 2013; Qian *et al.* 2013). The spike glycoprotein (spike) on the surface of SARS-CoV-2 is a viral fusogenic agent (Zhang *et al.* 2021). Spike interacts with the human angiotensin-converting enzyme 2 (hACE2) receptor at the target cell's surface. This process is marked as the first stage of the viral life cycle (V'kovski *et al.* 2021). Interaction between spike and hACE2 protein is followed by the activation of transmembrane protease serine 2 (TMPRSS2), which, in turn, fuse the viral membrane

* Corresponding Author

E-mail Address: enda041@brin.go.id

with the cellular membranes, and the deposition and uncoating of viral genomic RNA into the cellular cytoplasm (V'kovski *et al.* 2021). Most of the mutation of SARS-CoV-2 variants occur in the spike protein, which results in changes in hACE2 binding species-specificity (Meng *et al.* 2022). Furthermore, it has been reported that spike protein without any other viral protein could interact with hACE2 protein from neighbouring cells to promote cell-cell fusion or syncytium (Buchrieser *et al.* 2020; Rajah *et al.* 2021). Given that most current vaccines and other therapeutic options against SARS-CoV-2 are based on the spike protein.

Syncytia formation promotes viral transmission, immune evasion, and enhanced pathogenicity (Rajah *et al.* 2022). This cell phenomenon is strongly associated with severe cases of COVID-19 with extensive lung damage (Buchrieser *et al.* 2020; Bussani *et al.* 2020). It was confirmed by examining the histopathologic lung sections of patients who died from COVID-19, showing multinucleate pneumocytes with 2-20 nuclei (Braga *et al.* 2021). Consistently, *in vitro* analyses also showed that exogenous expression of spike, hACE2, and TMPRSS2 proteins leads to multinuclear syncytia in multiple cell lines (Lin *et al.* 2021; Braga *et al.* 2021; Suzuki *et al.* 2022). Although all SARS-CoV-2 variants are fusogenic, the spike protein of the B.1.617.2/Delta variant facilitates cell-cell fusion more efficiently than other variants (Saito *et al.* 2022).

A. paniculata, commonly known in Indonesia as sambiloto, is an herbaceous plant popularly used as traditional medicine for centuries in Asian countries (Nyeem *et al.* 2017). The pharmacological properties of *A. paniculata* are diverse and include antioxidant, anti-inflammatory, anticancer, antidiabetic, antimicrobial, and antiviral (Chao *et al.* 2021; Sa-Ngiamsuntorn *et al.* 2021; Li *et al.* 2022; Chau *et al.* 2024; Harikrishnan *et al.* 2023). *In vivo* and *in vitro* experiments have demonstrated that bioactive constituents of *A. paniculata* consist of andrographolide, neoandrographolide, and 14-deoxy-11,12-didehydroandrographolide exhibited antiviral activity for various viruses such as H5N1 virus, the human immunodeficiency virus (HIV), dengue virus, herpesvirus, and SARS-CoV-2 (Wiert *et al.* 2005; Uttakar *et al.* 2012; Sornpet *et al.* 2017; Paemanee *et al.* 2019; Jiang *et al.* 2021; Sa-Ngiamsuntorn *et al.* 2021).

The pharmacological properties of *A. paniculata* drive numerous studies to investigate its activity against SARS-CoV-2 infection. *In-silico* studies revealed that the activity and mechanism of *A. paniculata* bioactive compounds against virus proteins such as 3 L main protease (3CLpro), papain-like proteinase (PLpro), RNA-directed RNA polymerase (RdRp), spike protein, and also the virus receptor-binding domain of hACE2 (Murugan *et al.* 2021; Megantara *et al.* 2021). *In vitro* experiment demonstrated that *A. paniculata* extract and andrographolide exhibited vigorous inhibition activity against SARS-CoV-2 in human lung epithelial cells, Calu-3, with high safety and no apparent cytotoxicity (Sa-Ngiamsuntorn *et al.* 2021).

Despite this promising evidence, very few studies have experimentally explored the molecular mechanisms of *A. paniculata* extract against SARS-CoV-2 infections. Therefore, through this study, we investigated the potency of *A. paniculata* extract inhibiting the entry point of SARS-CoV-2. We utilized a non-virulent SARS-CoV-2 pseudovirus to mimic the native virus. Owing to its safety compared to the native virus, pseudovirus is designed for research purposes, particularly in BSL-2 facilities (Septisetyani *et al.* 2021). Furthermore, we perform *in vitro* analyses of syncytia formation mediated by SARS-CoV-2 spike. As the results, *A. paniculata* extract, especially at 10 µg/ml, showed a significant reduction in pseudovirus-infected cells and syncytia formation compared to the control cells, which in turn suggested that *A. paniculata* extract exhibited a potential antiviral activity against SARS-CoV-2.

2. Materials and Methods

2.1. Preparation of *A. paniculata* Extract

A. paniculata extract was purchased from a GMP-certified herbal product manufacturer in Indonesia as a concentrated extract packed in a soft capsule. As much as 100 mg of *A. paniculata* extract was dissolved in 1 ml of DMSO (Applichem, Germany) to make a 100 mg/ml stock solution. Then, the extract solution was centrifuged at 5,000 rpm for two minutes to separate the undissolved particles. Furthermore, the supernatant was taken and filtered with a 0.22 µm nylon filter (Himedia #SF127-50NO) and then stored at -20°C for further use.

2.2. Cell Culture and Reagents

The HEK293T cells obtained from ECACC (12022001) were cultured in High-Glucose Dulbecco's-modified Eagle's medium (DMEM) (Sigma-Aldrich, St. Louis USA) supplemented with 10% (v/v) of heat-inactivated fetal bovine serum (Sigma-Aldrich, St. Louis USA) and antibiotics (100 µg/ml streptomycin and 100 U/ml penicillin) (Sigma-Aldrich, #P4333). Cells were maintained in a 5% CO₂ incubator at 37°C. Cells at 70-80% confluency were then used for further experiments.

2.3. Cell Viability Assay

The effect of *A. paniculata* extract on HEK293T cell viability was evaluated using an MTT assay (Septisetiyan *et al.* 2014). The cells at a density of 8×10^4 cells per ml were seeded in a 96-well plate (Costar #3596, Corning). The next day, the cells were treated with *A. paniculata* extract at 0, 1, 10, and 100 µg/ml concentrations. Following incubation, the culture media containing *A. paniculata* extract were discarded, and then the cells were incubated for 2-3 hours with 100 µl of 0.5 µg/µL 3-(4,5-dimethylthiazol-2-yl)-2,5-diphenyltetrazolium bromide (MTT) containing culture medium (Sigma-Aldrich, St. Louis, USA). Viable cells would metabolize yellow dye MTT into bluish purple color formazan crystal. Then, the formazan was dissolved by adding 100 µl of DMSO and agitation at 100 rpm for 10 minutes. The absorbance of solubilized formazan was then measured at 570 nm using a microplate spectrophotometer (Multiskan GO, Thermo Scientific™). The treatment was conducted in triplicate. The percentage of cell viability was calculated according to the formula: $(OD_{\text{treated}} - OD_{\text{blank}}) / (OD_{\text{untreated}} - OD_{\text{blank}}) \times 100\%$.

2.4. Immunofluorescence staining

Coverslips with 14 mm diameter (NEST 801010) inside a 24-well plate (Costar #3526) were sterilized with 70% ethanol and coated with 2% gelatin. Then, HEK293T cell suspension at a density of 6×10^4 cells/ml was seeded on top of the coverslips. After overnight incubation, the cells were transfected with the pcDNA3.1-SARS2-Spike (a gift from Fang Li; Addgene #145032 (Shang *et al.* 2020)), pcDNA3.1-hACE (a gift from Fang Li; Addgene#145033 (Shang *et al.* 2020)), or TMPRSS2 (a gift from Roger Reeves; Addgene #53887 (Edie *et al.* 2018)) expression vectors by using polyethyleneimine (PEI) (PEI-MAX

24765-1, Polysciences, USA) in Opti-MEM reduced serum medium (Gibco 31085062, Thermo Fisher Scientific, USA). The next day, transfected cells were washed with 1X PBS and further incubated in the incubator for 24-48 hours.

At the end of incubation, the cells were washed with PBS and fixed with 4% paraformaldehyde (PFA) (Elabscience E-IR-R114, USA) for 10 min at room temperature. Cells were then incubated for 30 min to one hour at RT with blocking buffer (1% Bovine Serum Albumin (Sigma) in 1X PBS) and further incubated overnight at 4°C with anti-SARS-CoV-2 spike (Sino Biological #40150-R007), mouse anti-human ACE2 (R&D #MAB9332) or rabbit anti-TMPRSS2 (Novus Biologicals #NBP2-93322) antibodies diluted in blocking buffer (1:250). After incubation with the primary antibody, cells were washed three times with 1X PBS and incubated with secondary antibodies conjugated with Alexa Fluor 488 or Alexa Fluor 594 (Abcam #ab150080 or Abcam #ab150080) at a ratio of 1:1,000 in blocking buffer for 1 hour at RT. The secondary antibody was washed with 1X PBS three times. Finally, the cells were mounted with DAPI (4',6-diamidino-2-phenylindole)-containing mountant (Abcam #ab104139) to preserve the cells and stain the nuclei. The expression of recombinant proteins was observed and imaged using an Olympus IX83 motorized fluorescence microscope (Olympus, Tokyo, Japan).

2.5. SARS-CoV-2 Pseudotyping

Pseudotyping was performed based on Capcha *et al.* (2021) with modification. HEK293T cells were transfected with pcDNA3.1-SARS2-Spike to express SARS-CoV-2 spike transiently. The following day, the medium was removed and added with 3 ml medium containing pseudotyped G*ΔG-GFP rVSV (Kerafast EH1024-PM) at MOI ~3 to induce pseudotyping (Whitt 2010). One hour later, the medium was discarded, and the cells were fed with a new medium containing anti-VSV-G antibody at a ratio of 1:2,000 (Invitrogen, Thermo Fisher Scientific) and incubated overnight in the CO₂ incubator. The following day, the cell-conditioned medium supernatant containing pseudotyped spike*ΔG-GFP rVSV (SARS-CoV-2 pseudovirus) was collected after centrifugation to remove cell debris. Pseudovirus was aliquoted and stored at -80°C until further use.

2.6. Pseudovirus Entry Assay

The HEK293T cells were cultured at a density of 4×10^4 cells per well in an 8-well chamber slide (SPL Life Sciences, Pyeongtaek, South Korea), which was previously coated with 2% gelatin. After overnight incubation in a 5% CO₂ incubator at 37°C, the cells were co-transfected with 0.5 µg of pcDNA3.1-hACE2 and 0.5 µg of pcDNA3.1-TMPRSS2 plasmids using polyethylenimine (PEI) in Opti-MEM. The following day, the cells were pre-incubated with a complete medium containing *A. paniculata* extract at concentrations of 0, 1, or 10 µg/ml for 30 minutes. Then, the medium was removed, and the PSV was added at 1:2 ratios in 300 µL of medium containing *A. paniculata* extract with the same concentrations. After 16-18 h incubation, the cells were fixed with 4% PFA for 10 min at room temperature. After fixation, the cells were washed with 1XPBS and mounted with a DAPI-containing mounting medium. Infected cells were defined as cells with GFP spots and were observed using a motorized fluorescence microscope (Olympus IX83). The number of infected cells from 8 different microscope fields was quantified using Fiji software (National Institute of Health).

2.7. Syncytia Inhibition Assay

Syncytia inhibition assay was performed according to our previous publication (Septisetyani *et al.* 2024) with modification. The HEK293T cells at a density of 7×10^4 cells per well were seeded on a 24-well plate. The next day, the cells were co-transfected with three plasmids to express SARS-CoV-2 spike, hACE2, and TMPRSS2 recombinant proteins using PEI and incubated for about 6 hours. Following transfection, the cells were treated with *A. paniculata* extract at 0, 1, or 10 µg/ml concentrations and incubated for about 16-18 hours. Syncytia formation was observed using an inverted microscope (Olympus CKX53), and a total of 20 images from two wells were acquired. The total number of syncytia was calculated with Fiji software and then sorted based on the number of nuclei using four categories: (i) <5 nuclei, (ii) 6-10 nuclei, (iii) 11-15 nuclei, and (iv) >15 nuclei.

2.8. Statistical Analysis

All statistical analyses were performed using Microsoft Excel and One-way ANOVA with Tukey's post hoc test using SPSS version 26.

3. Results

3.1. *A. paniculata* Extract Exhibits Safety and Non-toxic Concentrations on HEK293 Cells

In this study, we aimed to investigate the anti-SARS-CoV-2 activity of *A. paniculata* extract without causing cytotoxicity to the host cells. To do that, we first examined the viability of HEK293 cells after 24 h treatment with a series of concentrations of *A. paniculata* extract (0, 1, 10, and 100 µg/ml). As a result, cells treated with 1 and 10 µg/ml extract exhibited 97.96±3.99% and 95.24±3.82% cell viability (Figure 1A), respectively, indicating no toxic effect of *A. paniculata* extracts. Moreover, the 100 µg/ml of *A. paniculata* extract caused the cell viability to drop to 75.04±6.14% (Figure 1A), and the cells showed abnormal morphology such as shrinking, rounding, and detachment from the culture vessel (Figure 1B). Based on these findings, we concluded that 1 and 10 µg/ml of *A. paniculata* extract are non-cytotoxic concentrations on the viability of the HEK293T cells.

3.2. *A. paniculata* Extract Inhibits Cellular Entry of SARS-CoV-2 Pseudovirus

Using the SARS-CoV-2 pseudovirus system with rVSV backbone, we demonstrated the inhibition of *A. paniculata* extract on SARS-CoV-2 pseudovirus entry in recombinant HEK293T cells. At first, we investigated the exogenous expression of spike, hACE2, and TMPRSS2 in HEK293T cells to check the functionality of the expression vectors (Figure 2A-C). As the results, we observed the expression of those recombinant proteins using immunofluorescence staining. After we confirmed the expression of hACE2 and TMPRSS2 in HEK293T cells (Figure 2B and C), we used the co-transfected cells for pseudovirus entry assay and infected the cells with pseudotyped spike*ΔG-GFP, resulting in the GFP dots detection around the nuclei within cultured cells (Figure 3A, white arrows). Interestingly, the addition of 10 µg/ml of *A. paniculata* extract reduced the percentage of the infected cell number with GFP dots (6.67±4.78%) ($P = 0.02$). In comparison, one µg/ml of extract did not significantly reduce the number of infected cells (11.16±4.67%) ($P = 0.26$) compared to the control cells (14.73±7.31%) (Figure 3B). These data indicated that the inhibition effect of *A. paniculata* extract towards

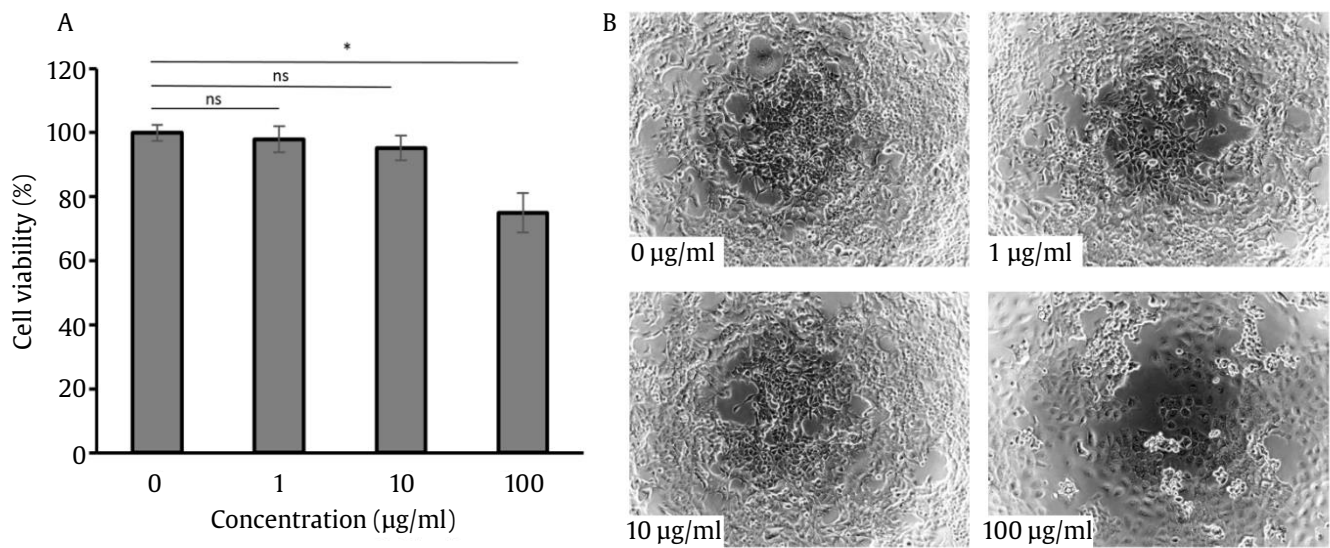


Figure 1. The viability profiles of HEK293T cells after 24 h of treatment with *A. paniculata* extract. (A) The graph shows the cell viability (%) profile after treatment with 0, 1, 10, and 100 µg/mL of *A. paniculata* extract. (B) Representative images show the morphology of HEK293T cells after 24 h treatment with *A. paniculata* extract (n=3). Data represent \pm SD, * p <0.05 (One-way ANOVA with Tukey's test)

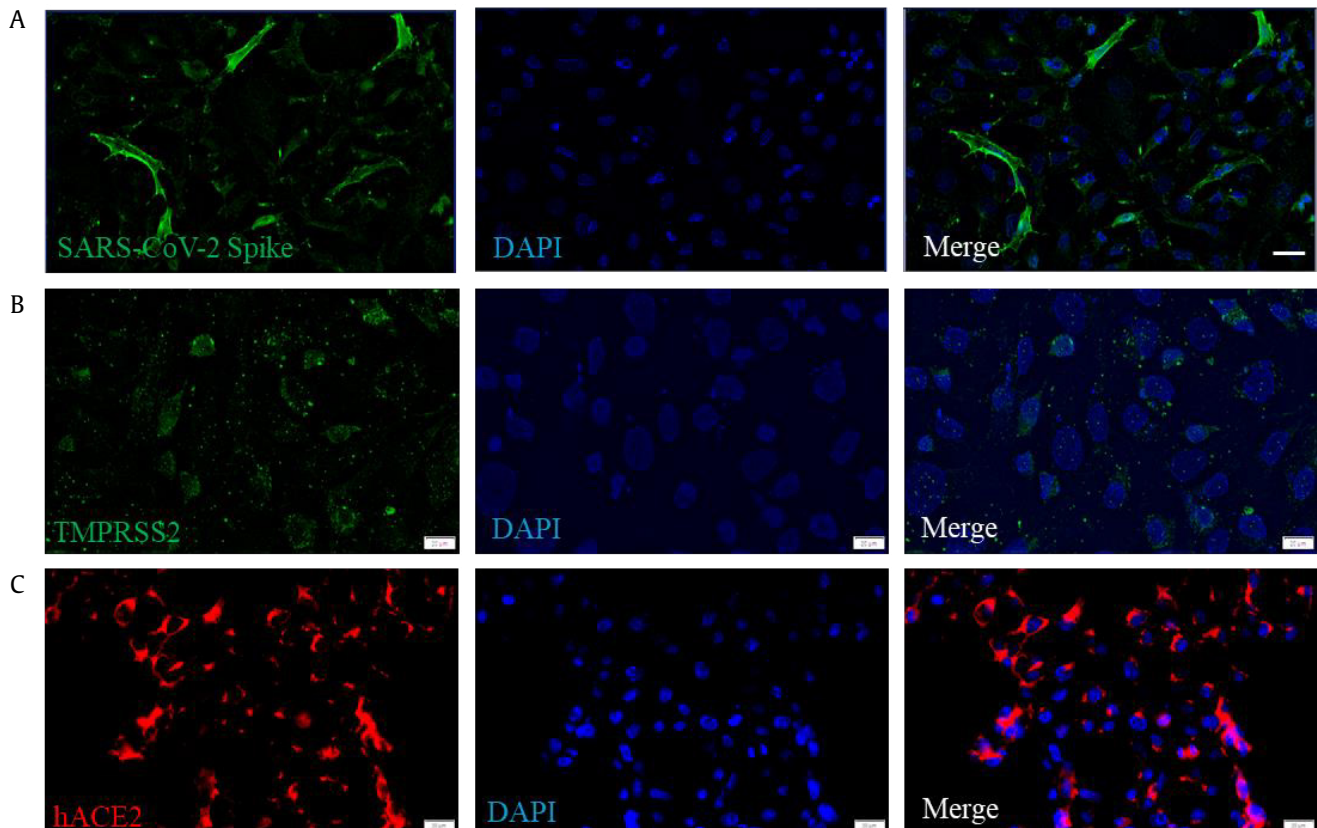


Figure 2. Fluorescence images of HEK293T cells expressing spike, TMPRSS2, and hACE2 stained with anti-spike, anti-TMPRSS2, and anti-hACE antibodies, respectively. Spike (A) and TMPRSS2 (B) proteins were visualized with Alexa-488 (green), while the hACE receptor (C) protein was detected with Alexa-594 (red). Nucleus were stained with DAPI (blue). Scale bars, 20 µm

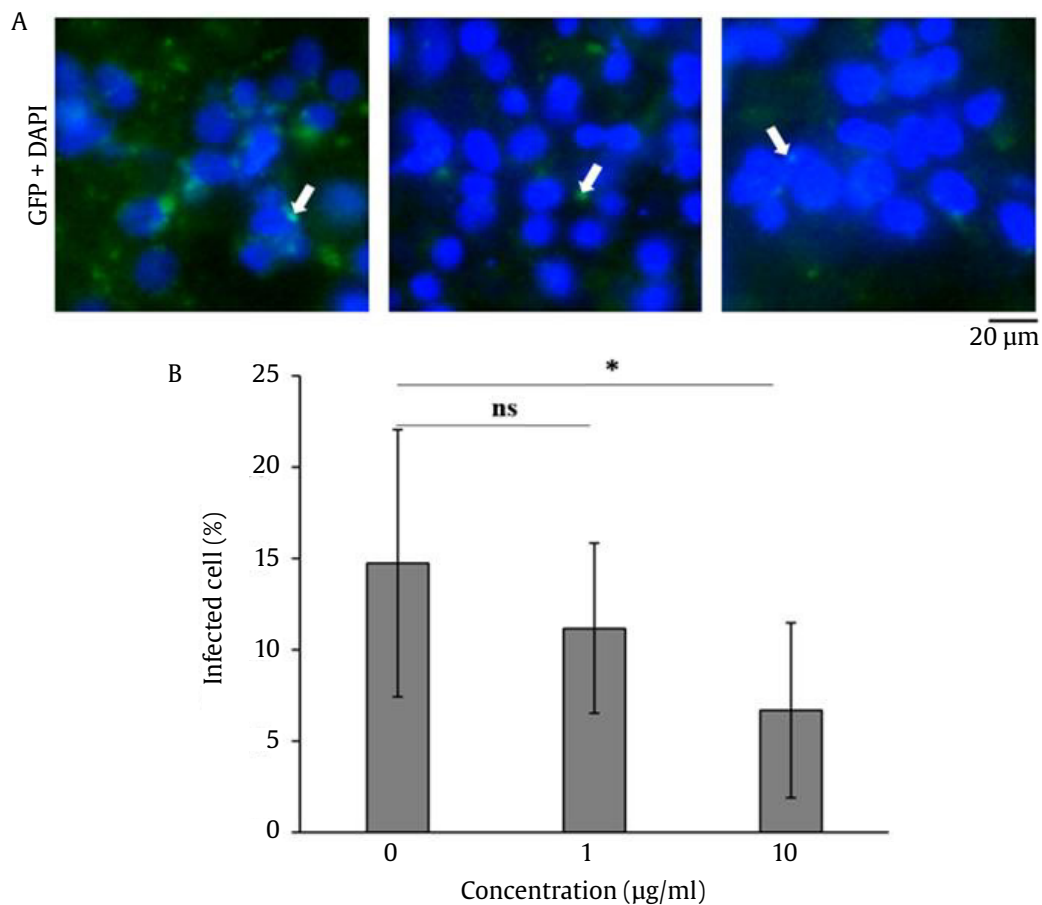


Figure 3. Antiviral activity of *A. paniculata* extracts against SARS-CoV-2 pseudovirus cellular entry in HEK293T cells expressing hACE2/TMPRSS2. (A) Fluorescence images of the HEK293T cells co-expressing hACE2/TMPRSS2 after infected with pseudotyped SARS-CoV-2 spike*ΔG-GFP. The infected cell is indicated by GFP spots around the nucleus (white arrows). The blue color indicates nucleus staining by DAPI. Scale bars = 20 µm. (B) The graph shows the statistical analysis of the number of infected cells. Data represent means ±SD, * $p < 0.05$ (One-way ANOVA with Tukey's test)

SARS-CoV-2 entry is a concentration-dependent inhibition.

3.3. *A. paniculata* Extract Inhibits the Syncytia Formation in HEK293T Cells

We have found that *A. paniculata* extract has antiviral activity by inhibiting SARS-CoV-2 pseudovirus cellular entry in HEK293T cells transfected with hACE2/TMPRSS2. To further investigate whether *A. paniculata* extract also leads to the reduction of syncytia formation as the marker of the severely damaged lung of COVID-19 patients, we co-expressed spike, hACE2, and TMPRSS2 in HEK293T cells to induce *in vitro* syncytia formation. We confirmed the exogenous expression of the recombinant proteins in HEK293T cells using immunostaining analyses (Figure 2). Furthermore,

we observed that the HEK293T cells transfected with spike, hACE2, and TMPRSS2 expression vectors formed multinucleated cells due to cell-cell fusion as determined by brightfield image analyses (Figure 4B; red dashed lines). Interestingly, adding 1 and 10 µg/ml of *A. paniculata* extract blocked the cell-cell fusion by reducing the number of syncytia formations with syncytia numbers 17.2 ($P < 0.001$) and 19.9 ($P < 0.001$) compared to control cells (29.85). Moreover, treating cells, especially with ten µg/ml of *A. paniculata* extract, significantly reduces the number of nuclei observed within syncytia with the number of nuclei <5, 6-10, 10-15, and >15 were 1.7 ($P = 0.006$), 4.75 ($P \leq 0.0002$), 5.15 ($P = 0.49$), and 5.6 ($P = 0.004$) compared to control cells (3.52, 9.42, 5.71, and 11.19) (Figure 4A).

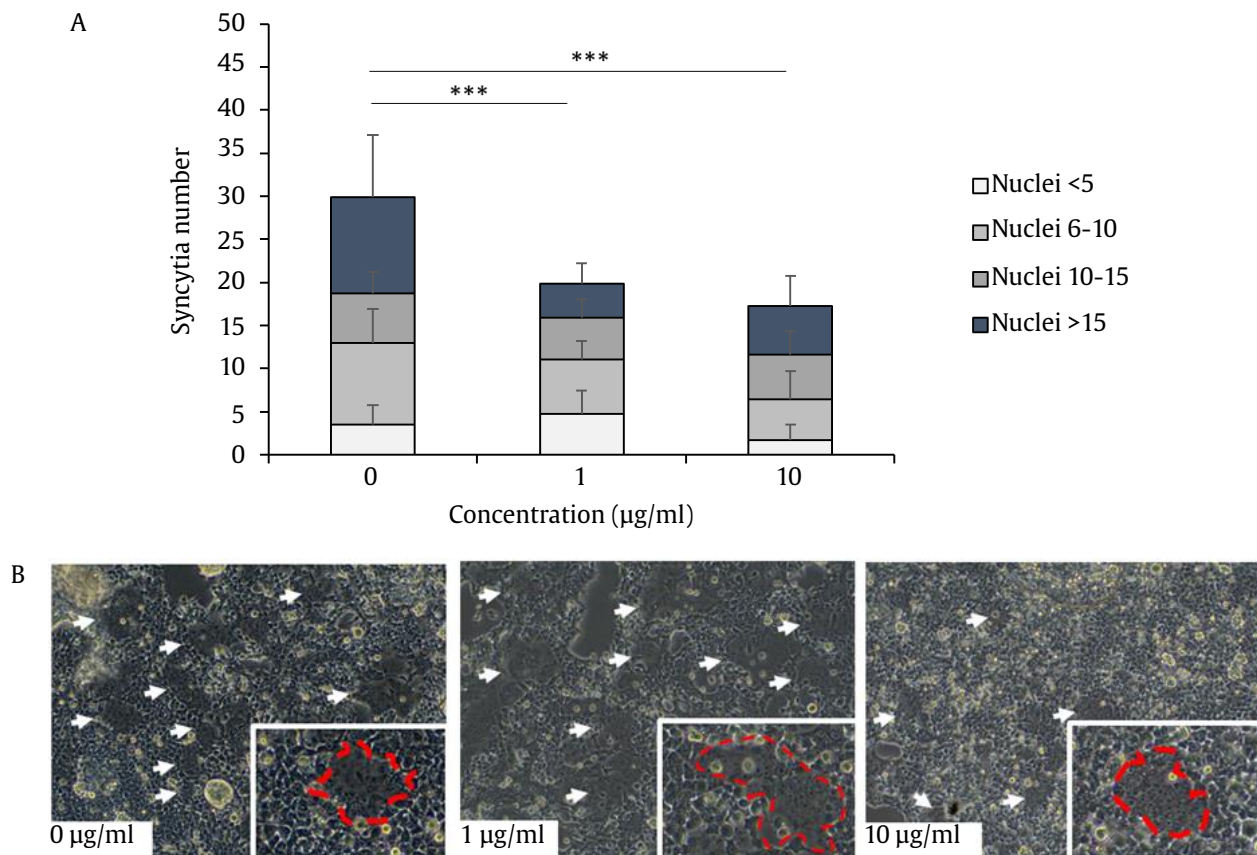


Figure 4. The effect of *A. paniculata* extract on the formation of syncytia. (A) The graph shows the statistical analysis of syncytia at 0, 1, and 10 µg/ml of *A. paniculata* extract. Data represent means \pm SD (n = 20 microscope fields of two wells), *** = $p < 0.001$ (One-way ANOVA with Tukey's test). (B) The brightfield images of syncytia formation in HEK293T cells transfected with spike, hACE2, and TMPRSS2 expression vectors in the presence of 0, 1, and 10 µg/ml of *A. paniculata* extract. Scale bars, 20 µm

4. Discussion

At the beginning of this study, we demonstrated that one µg/ml and ten µg/ml of *A. paniculata* extract are the safest and have no significant toxicity on the viability of HEK293T cells. Interestingly, ten µg/ml of *A. paniculata* extract shows a potential inhibition activity of *A. paniculata* extract on pseudovirus SARS-CoV-2 entry to the host cells. In line with this result, a previous study also confirmed that *A. paniculata* extract showed a high therapeutic index of SARS-CoV-2 antiviral activity with minimal cell toxicity in cells representing five major organs, including the liver (HepG2 and imHC), kidney (HK-2), intestine (Caco-2), lung (Calu-3), and brain (SH-SY5Y) (Sangiampurno *et al.* 2021). It is essential for a study to establish the antiviral activity at a concentration that does not induce toxicity to the cells (Mukherjee 2019).

Pseudoviruses (or pseudotyped viruses) are recombinant viruses structured with a core or backbone and surface protein derived from different viral origins. In addition, pseudoviruses are powerful systems, particularly in an attempt to investigate the infection mechanism of highly infectious viruses such as SARS-CoV-2. The pseudovirus system can overcome the difficulty of requiring sophisticated facilities, such as BSL-3, for highly infectious viral experiments involving virus propagation (Septisetiyaningrum *et al.* 2021). Therefore, to explore the antiviral activity of *A. paniculata* extract on SARS-CoV-2 cellular entry, we utilized the pseudovirus constructed with vesicular stomatitis virus (VSV) backbone incorporating green fluorescence protein (GFP) gene reporter and spike surface protein from SARS-CoV-2 (rVSV Δ G-GFP system). Thus, GFP-positive cells indicated the successful infection of

pseudotyped rVSV in the target cells (Fukushi *et al.* 2008; Figure 3A, white arrows). It has been known that the entry process of SARS-CoV-2 is initiated with the interaction between the hACE2 receptor and SARS-CoV-2 spike proteins at the surface of target cells (V'kovski *et al.* 2021). Interaction between spike and hACE2 is followed by the activation of TMPRSS2, which, in turn, induces the fusion of the viral membrane with the cellular membrane, followed by the deposition and uncoating of viral genomic RNA into the cellular cytoplasm (V'kovski *et al.* 2021). Therefore, numerous pharmacological studies targeted spike proteins to inhibit these early stages of SARS-CoV-2 life cycles (Bojadzic *et al.* 2021; Wang *et al.* 2021; Cheke *et al.* 2021; Shin *et al.* 2022).

The present study utilized a pseudovirus system to investigate the effect of *A. paniculata* in inhibiting virus entry in HEK293T cells transfected with recombinant plasmids to express hACE2 and TMPRSS2. We found that ten µg/ml extract showed entry inhibition of SARS-CoV-2 pseudovirus. This finding is the first evidence that experimentally reported that *A. paniculata* extract could inhibit the process of entry virus using a pseudovirus system. Previously, Sa-ngiamsuntorn *et al.* (2021) reported that *A. paniculata* extract is more potent in inhibiting the SARS-CoV-2 virus during viral assembly and maturation. They also suggest that *A. paniculata* extract may block the virus entry. Moreover, *in silico* docking study demonstrated that bioactive secondary metabolites from *A. paniculata* such as andrographolide, neoandrographolide, andrographic acid, 14-deoxyandrographolide, 14-deoxy 11, 12-didehydroandrographolide, 3, 4-dicaffeoylquinic acid, onysilin, 14-deoxy 14, 15-dehydroandrographolide, 7-O-methylgonin, andrograponin and 19-O-acetyl-14-deoxy 11,12-didehydroandrographolide possess high binding affinity towards SARS-CoV-2 receptor, suggesting that *A. paniculata* is potential to inhibit SARS-CoV-2 at the initial stages of infection (Sahitya *et al.* 2021).

SARS-CoV-2 is a respiratory syncytial virus (RSV) that causes infected lung and respiratory tract cells to fuse, resulting in multinucleated cells called syncytia (Buchrieser *et al.* 2020). Syncytia formation in the cells infected by SARS-CoV-2 potentially facilitates viral replication, dissemination, and severe tissue damage (Leroy *et al.* 2020). This study demonstrated that *A. paniculata* extract, at

concentrations of one µg/ml and ten µg/ml, might inhibit SARS-CoV-2 spreading by reducing the syncytia number in HEK293T cells transfected with spike, hACE2, and TMPRSS2 expression vectors.

Syncytia formation is considered one of the hallmarks of severe COVID-19 cases. Several studies have shown the presence of giant multinucleated syncytia in the lungs of severe COVID-19 patients (Franks *et al.* 2003; Nicholls *et al.* 2003; Chan *et al.* 2013; Xu *et al.* 2020). Our *in vitro* study showed that co-transfection of HEK293T cells with spike, hACE2, and TMPRSS2 encoding plasmids promotes cell-cell fusion, which plays an *in vitro* model for syncytia formation study. Interestingly, our current study showed for the first time that adding *A. paniculata* to this culture system could reduce the number of cell-cell fusion, as determined by brightfield image analysis. A previous study reported that methanol extract of *A. paniculata* suppressed syncytia formation in co-cultures of HIV-1 infected MOLT cell line (Otake *et al.* 1955). How *A. paniculata* extract reduced the formation of syncytia is still unclear. More studies are needed to demonstrate the mechanism of *A. paniculata* extract in inhibiting the formation of SARS-CoV-2-mediated syncytia.

A. paniculata extract may reduce syncytia formation by modulation of spike protein-mediated syncytia formation. After viral entry and taking over the transcription and translation machinery of the cell host, the newly transcribed spike protein is transported to the cell's plasma membrane throughout the ER-Golgi network. The spike protein at the cell surface interacts with the hACE2 protein on neighbouring cells, triggering syncytia generation (Rajah *et al.* 2022). Furthermore, heparan sulfate proteoglycan (HSPG), a class of negative charge-enriched polysaccharides at the cell surface, induces hACE2 clustering and facilitates spike-induced cell-cell fusion (Zhang *et al.* 2023). In contrast, a study revealed that the spike protein-induced cell-cell fusion is independent of the hACE2 protein and requires proteasomal cleavage of the spike. At the same time, TMPRSS2 is unnecessary for this mechanism (Reuter *et al.* 2023). Since the present data is the first demonstration of *A. paniculata* extracts inhibiting the syncytia formation during SARS-CoV-2 infection, it is necessary to investigate the molecular mechanisms of antiviral activities of *A. paniculata* extracts and its bioactive compounds in reducing the formation of syncytia.

In conclusion, this study reveals the potency of *A. paniculata* extract as an herbal-derived antiviral agent against SARS-CoV-2 infection. Our study is the first to use SARS-CoV-2 pseudovirus as a model to examine the effect of *A. paniculata* extract on SARS-CoV-2 infection and use the syncytia assay to investigate its potential inhibition of viral cell-to-cell transmission. Our findings suggest that *A. paniculata* extract may inhibit the cellular entry of SARS-CoV-2 and reduce the severity of lung damage in COVID-19 patients.

Considering that COVID-19 has become an endemic disease, while the supply of its medicines is still limited, alternative therapies are needed, one of which is herbal supplement-based therapy. Furthermore, *A. paniculata* extract could be an alternative therapeutic agent for hindering SARS-CoV-2 infection and reducing the severity of COVID-19 progression. *A. paniculata* extract can be used as an herbal supplement with andrographolide content of the extract used for standardization of the product. Wanaratna *et al.* 2022 has been reported the potency of standardized *A. paniculata* extract that contains 20 mg andrographolide per capsule to treat patients with mild COVID-19. In addition, consumption of the extract up to thrice daily (60 mg andrographolide per day) for 5 days has not exhibited observable hepatic or renal impairments. Finally, the production of herbal supplements must, of course, follow the local regulatory agencies to ensure product quality and safety.

Acknowledgements

This research was financially supported by grant no. 102/FI/P-KCOVID-19.2B3/IX/2020 from LPDP/BRIN and RIIM No. KEP-5/LPDP/LPDP.4/2022 from the Research Organization for Life Sciences and Environment, National Research and Innovation Agency (Research Program 2022).

References

- Afifa, 2023. Jakarta Health Office Confirms 80 COVID-19 Cases between November and December. Available at: <https://en.tempco.co/read/1807260/jakarta-health-office-confirms-80-covid-19-cases-between-november-and-december>. [Date access: 9 December 2023]
- Braga, L., Ali, H., Secco, I., Chiavacci, E., Neves, G., Goldhill, D., Penn, R., Jimenez-Guardeño, J.M., Ortega-Prieto, A.M., Bussani, R., Cannatà, A., 2021. Drugs that inhibit TMEM16 proteins block SARS-CoV-2 spike-induced syncytia. *Nature*. 594, 88-93. <https://doi.org/10.1038/s41586-021-03491-6>
- Buchrieser, J., Dufloo, J., Hubert, M., Monel, B., Planas, D., Rajah, M.M., Planchais, C., Porrot, F., Guivel-Benhassine, F., Van der Werf, S., Casartelli, N., 2020. Syncytia formation by SARS-CoV-2-infected cells. *EMBO J.* 39, p.e106267. <https://doi.org/10.15252/emboj.2020106267>
- Bussani, R., Schneider, E., Zentilin, L., Collesi, C., Ali, H., Braga, L., Volpe, M.C., Colliva, A., Zanconati, F., Berlot, G. and Silvestri, F., 2020. Persistence of viral RNA, pneumocyte syncytia and thrombosis are hallmarks of advanced COVID-19 pathology. *EBioMedicine*. 61, 103-104. <https://doi.org/10.1016/j.ebiom.2020.103104>
- Bojadzic, D., Alcazar, O., Chen, J., Chuang, S.T., Condor Capcha, J.M., Shehadeh, L.A. and Buchwald, P., 2021. Small-molecule inhibitors of the coronavirus spike: ACE2 protein-protein interaction as blockers of viral attachment and entry for SARS-CoV-2. *ACS Infect. Dis.* 7, 1519-1534. <https://doi.org/10.1021/acinfecdis.1c00070>
- Capcha CJM, Lambert G, Dykxhoorn DM, Salerno AG, Hare JM, Whitt MA, Pahwa S, Jayaweera DT, Shehadeh LA. 2021. Generation of SARS-CoV-2 spike pseudotyped virus for viral entry and neutralization assays: A 1-week protocol. *Front. Cardiovasc. Med.* 7, 618651. DOI: 10.3389/fcvm.2020.618651. <https://doi.org/10.3389/fcvm.2020.618651>
- Chan, J.F.W., Chan, K.H., Choi, G.K.Y., To, K.K.W., Tse, H., Cai, J.P., Yeung, M.L., Cheng, V.C.C., Chen, H., Che, X.Y. and Lau, S.K.P., 2013. Differential cell line susceptibility to the emerging novel human betacoronavirus 2c EMC/2012: implications for disease pathogenesis and clinical manifestation. *J. Infect. Dis.* 207, 1743-1752. <https://doi.org/10.1093/infdis/jit123>
- Che, S., Zhou, N., Liu, Y., Xie, J. and Liu, E., 2023. Andrographolide exerts anti-respiratory syncytial virus activity by up-regulating heme oxygenase-1 independent of interferon responses in human airway epithelial cells. *Mol. Biol. Rep.* 50, 4261-4272. <https://doi.org/10.1007/s11033-023-08346-z>
- Cheke, R.S., Narkhede, R.R., Shinde, S.D., Ambhore, J.P. and Jain, P.G., 2021. Natural product emerging as potential SARS spike glycoproteins-ACE2 inhibitors to combat COVID-19 attributed by in-silico investigations. *Biointerface Res. Appl. Chem.* 11, 10628-10639. <https://doi.org/10.33263/BRIAC113.1062810639>
- Chau, T.P., Devanesan, S., Ayub, R. and Perumal, K., 2024. Identification and characterization of major bioactive compounds from *Andrographis paniculata* (Burm. f.) extracts showed multi-biomedical applications. *Environ. Res.* 242, 117763. <https://doi.org/10.1016/j.envres.2023.117763>
- Chao, W.W., Kuo, Y.H., Lin, B.F., 2021. Isolation and identification of *Andrographis paniculata* (Chuanxinlian) and its biologically active constituents inhibited enterovirus 71-induced cell apoptosis. *Front. Pharmacol.* 12, 762285. <https://doi.org/10.3389/fphar.2021.762285>
- Dominguez, S.R., Travanty, E.A., Qian, Z. and Mason, R.J., 2013. Human coronavirus HKU1 infection of primary human type II alveolar epithelial cells: cytopathic effects and innate immune response. *PLoS One*. 8, e70129. <https://doi.org/10.1371/journal.pone.0070129>
- Edie, S., Zaghoul, N.A., Leitch, C.C., Klinedinst, D.K., Lebron, J., Thole, J.F., McCallion, A.S., Katsanis, N., Reeves, R.H., 2018. Survey of human chromosome 21 gene expression effects on early development in *Danio rerio*. *G3 (Bethesda)*. 8, 2215-2223. DOI: 10.1534/g3.118.200144. <https://doi.org/10.1534/g3.118.200144>

- Fukushi, S., Watanabe, R., Taguchi, F., 2008. Pseudotyped vesicular stomatitis virus for analysis of virus entry mediated by SARS coronavirus spike proteins. In: Cavanagh D (Eds.). *SARS- and Other Coronaviruses. Methods in Molecular Biology, Vol 454*. Totowa, NJ: Humana Press. pp. 331-338. https://doi.org/10.1007/978-1-59745-181-9_23
- Franks, T.J., Chong, P.Y., Chui, P., Galvin, J.R., Lourens, R.M., Reid, A.H., Selbs, E., Mcevoy, C.P.L., Hayden, C.D.L., Fukuoka, J., Taubenberger, J.K., 2003. Lung pathology of severe acute respiratory syndrome (SARS): a study of 8 autopsy cases from Singapore. *Hum. Pathol.* 34, 743-748. [https://doi.org/10.1016/S0046-8177\(03\)00367-8](https://doi.org/10.1016/S0046-8177(03)00367-8).
- Harikrishnan, A., Veena, V., Kancharla, R., Chavan, S., Rajabathar, J.R., Al-Lohedan, H., Pandiaraj, S., Karuppiyah, P., Arokiyaraj, S., 2023. Anti-breast cancer activity of bioactive metabolites from *Andrographis paniculata* through inhibition of PI3K activity in triple negative breast cancer (MDA-MB-231) cells. *J. Mol. Struct.* 1294, 136506. <https://doi.org/10.1016/j.molstruc.2023.136506>
- Jiang, M., Sheng, F., Zhang, Z., Ma, X., Gao, T., Fu, C. and Li, P., 2021. *Andrographis paniculata* (Burm. f.) nees and its major constituent andrographolide as potential antiviral agents. *J. Ethnopharmacol.* 272, 113954. <https://doi.org/10.1016/j.jep.2021.113954>
- Leroy, H., Han, M., Woottum, M., Bracq, L., Bouchet, J., Xie, M. and Benichou, S., 2020. Virus-mediated cell-cell fusion. *Int. J. Mol. Sci.* 21, 9644. <https://doi.org/10.3390/ijms21249644>
- Li, X., Yuan, W., Wu, J. and Zhen, J., 2022. Andrographolide, a natural anti-inflammatory agent: an update. *Front. Pharmacol.* 13, 920435. <https://doi.org/10.3389/fphar.2022.920435>
- Lin, L., Li, Q., Wang, Y., Shi, Y., 2021. Syncytia formation during SARS-CoV-2 lung infection: a disastrous unity to eliminate lymphocytes. *Cell Death. Differ.* 28, 2019-2021. <https://doi.org/10.1038/s41418-021-00795-y>
- Megantara, S., Levita, J., Ibrahim, S., Nguyen, B.P., 2021. Andrographolide, a diterpenoid lactone compound of *andrographis paniculata*, binds to lys353 and asp38 in the peptidase domain of human angiotensin-converting enzyme 2. *Rasayan J. Chem.* 14, 241-247. <http://doi.org/10.31788/RJC.2021.1416070>
- Meng, B., Datir, R., Choi, J., Baker, S., Dougan, G., Hess, C., Kingston, N., Lehner, P.J., Lyons, P.A., Matheson, N.J., Owehand, W.H., 2022. SARS-CoV-2 spike N-terminal domain modulates TMPRSS2-dependent viral entry and fusogenicity. *Cell Rep.* 40, 111220. <https://doi.org/10.1016/j.celrep.2022.111220>
- Mukherjee, P.K., 2019. Antiviral evaluation of herbal drugs, in: Mukherjee, P.K. (Eds.), *Quality Control and Evaluation of Herbal Drugs*. Elsevier, p. 599. <https://doi.org/10.1016/B978-0-12-813374-3.00016-8>
- Murugan, N.A., Pandian, C.J., Jeyakanthan, J., 2021. Computational investigation on *Andrographis paniculata* phytochemicals to evaluate their potency against SARS-CoV-2 in comparison to known antiviral compounds in drug trials. *J. Biomol. Struct. Dyn.* 39, 4415-4426. <https://doi.org/10.1080/07391102.2020.1777901>
- Nicholls, J.M., Poon, L.L., Lee, K.C., Ng, W.F., Lai, S.T., Leung, C.Y., Chu, C.M., Hui, P.K., Mak, K.L., Lim, W., Yan, K.W., 2003. Lung pathology of fatal severe acute respiratory syndrome. *Lancet.* 361, 1773-1778. [https://doi.org/10.1016/S0140-6736\(03\)13413-7](https://doi.org/10.1016/S0140-6736(03)13413-7)
- Nyeem, M.A.B., Mannan, M.A., Nuruzzaman, M., Kamrujjaman, K.M., Das, S.K., 2017. Indigenous king of bitter (*Andrographis paniculata*): a review. *J. Med. Plants Stud.* 5, 318-324.
- Otake, T., Mori, H., Morimoto, M., Ueba, N., Sutardjo, S., Kusumoto, I.T., Hattori, M., Namba, T., 1995. Screening of Indonesian plant extracts for anti-human immunodeficiency virus-type 1 (HIV-1) activity. *Phytother. Res.* 9, 6-10. <https://doi.org/10.1002/ptr.2650090103>
- Paemane, A., Hitakarun, A., Wintachai, P., Roytrakul, S., Smith, D.R., 2019. A proteomic analysis of the anti-dengue virus activity of andrographolide. *Biomed. Pharmacother.* 109, 322-332. <https://doi.org/10.1016/j.biopha.2018.10.054>
- Qian, Z., Dominguez, S.R. and Holmes, K.V., 2013. Role of the spike glycoprotein of human Middle East respiratory syndrome coronavirus (MERS-CoV) in virus entry and syncytia formation. *PLoS One.* 8, e76469. <https://doi.org/10.1371/journal.pone.0076469>
- Rajah, M.M., Hubert, M., Bishop, E., Saunders, N., Robinot, R., Grzelak, L., Planas, D., Dufloo, J., Gellenoncourt, S., Bongers, A., Zivaljic, M., 2021. SARS-CoV-2 alpha, beta, and delta variants display enhanced spike-mediated syncytia formation. *The EMBO J.* 40, e108944. <https://doi.org/10.15252/embj.2021108944>
- Rajah, M.M., Bernier, A., Buchrieser, J., Schwartz, O., 2022. The mechanism and consequences of SARS-CoV-2 spike-mediated fusion and syncytia formation. *J. Mol. Biol.* 434, 167280. <https://doi.org/10.1016/j.jmb.2021.167280>
- Reuter, N., Chen, X., Kropff, B., Peter, A.S., Britt, W.J., Mach, M., Überla, K., Thomas, M., 2023. SARS-CoV-2 spike protein is capable of inducing cell-cell fusions independent from its receptor ACE2 and this activity can be impaired by furin inhibitors or a subset of monoclonal antibodies. *Viruses*, 15, 1500. <https://doi.org/10.3390/v15071500>
- Sahithya, M.D., Srinath, M., Kumar, B.C. and Giri, C.C., 2021. Molecular *in silico* docking interventions in various SARS-CoV-2 receptor targets involving bioactive herbal compounds of *Andrographis paniculata* (Burm. f.) Nees. *Ann. Phytomed.* 10, 22-39, <https://doi.org/10.21276/ap.covid19.2021.10.1.4>
- Sa-Ngiamsuntorn, K., Suksatu, A., Pewkliang, Y., Thongsri, P., Kanjanasirirat, P., Manopwisedjaroen, S., Charoensutthivarakul, S., Wongtrakoonate, P., Pitiporn, S., Chaopreecha, J., Kongsomros, S., 2021. Anti-SARS-CoV-2 activity of *Andrographis paniculata* extract and its major component andrographolide in human lung epithelial cells and cytotoxicity evaluation in major organ cell representatives. *J. Nat. Prod.* 84, 1261-1270. <https://doi.org/10.1021/acs.jnatprod.0c01324>
- Saito, A., Irie, T., Suzuki, R., Maemura, T., Nasser, H., Uriu, K., Kosugi, Y., Shirakawa, K., Sadamasu, K., Kimura, I., Ito, J., 2022. Enhanced fusogenicity and pathogenicity of SARS-CoV-2 delta P681R mutation. *Nature.* 602, 300-306. <https://doi.org/10.1038/s41586-021-04266-9>
- Septisetyani, E.P., Ningrum, R.A., Romadhani, Y., Wisnuwardhani, P.H., Santoso, A., 2014. Optimization of sodium dodecylsulphate as a formazan solvent and comparison of 3-(4,-5-dimethylthiazo-2-yl)-2,5-diphenyltetrazolium bromide (MTT) assay with WST-1 assay in MCF-7 cells, *Indones. J. Pharm.* 25, 245. <https://doi.org/10.14499/indonesianjpharm25iss4pp245>
- Septisetyani, E.P., Prasetyaningrum, P.W., Anam, K., Santoso, A., 2021. SARS-CoV-2 antibody neutralization assay platforms based on epitopes sources: live virus, pseudovirus, and recombinant S glycoprotein RBD. *Immune Netw.* 21, e39. <https://doi.org/10.4110/in.2021.21.e39>

- Septisetyani, E.P., Prasetyaningrum, P.W., Paramitasari, K.A., Suyoko, A., Himawan, A.L.I., Azzahra, S., Wisnuwardhani, P.H., Anam, K., Ramadani, R.D., Santoso, A., Ningrum, R.A., Herawati, N., Rubiyana, Y., 2024. Naringin effect on SARS-CoV-2 pseudovirus entry and spike mediated syncytia formation in hACE2-overexpressing cells. *HAYATI J. Biosci.* 31, 336-347. <https://doi.org/10.4308/hjb.31.2.336-347>
- Shang, J., Ye, G., Shi, K., Wan, Y., Luo, C., Aihara, H., Geng, Q., Auerbach, A., Li, F., 2020. Structural basis of receptor recognition by SARS-CoV-2. *Nature.* 581, 221-224. DOI: 10.1038/s41586-020-2179-y. <https://doi.org/10.1038/s41586-020-2179-y>
- Shin, Y.H., Jeong, K., Lee, J., Lee, H.J., Yim, J., Kim, J., Kim, S., Park, S.B., 2022. Inhibition of ACE2-spike interaction by an ACE2 binder suppresses SARS-CoV-2 entry. *Angewandte Chemie.* 134, e202115695. <https://doi.org/10.1002/anie.202115695>
- Siridechakorn, I., Bhattarakosol, P., Sasivimolrattana, T., Anoma, S., Wongwad, E., Nuengchamnong, N., Kowitdamrong, E., Boonyasuppayakorn, S., Waranuch, N., 2023. Inhibitory efficiency of *Andrographis paniculata* extract on viral multiplication and nitric oxide production. *Sci. Rep.* 13, 19738. <https://doi.org/10.1038/s41598-023-46249-y>
- Suzuki, R., Yamasoba, D., Kimura, I., Wang, L., Kishimoto, M., Ito, J., Morioka, Y., Nao, N., Nasser, H., Uriu, K., Kosugi, Y., 2022. Attenuated fusogenicity and pathogenicity of SARS-CoV-2 omicron variant. *Nature.* 603, 700-705. <https://doi.org/10.1038/s41586-022-04462-1>
- Sornpet, B., Potha, T., Tragoolpua, Y. and Pringproa, K., 2017. Antiviral activity of five Asian medicinal plant crude extracts against highly pathogenic H5N1 avian influenza virus. *Asian Pac. J. Trop. Med.* 10, 871-876. <https://doi.org/10.1016/j.apjtm.2017.08.010>
- Uttekar, M.M., Das, T., Pawar, R.S., Bhandari, B., Menon, V., Gupta, S.K., Bhat, S.V., 2012. Anti-HIV activity of semisynthetic derivatives of andrographolide and computational study of HIV-1 gp120 protein binding. *Eur. J. Med. Chem.* 56, 368-374. <https://doi.org/10.1016/j.ejmech.2012.07.030>
- V'kovski, P., Kratzel, A., Steiner, S., Stalder, H. and Thiel, V., 2021. Coronavirus biology and replication: implications for SARS-CoV-2. *Nat. Rev. Microbiol.* 19, 155-170. <https://doi.org/10.1038/s41579-020-00468-6>
- Wanaratna, K., Leethong, P., Inchai, N., Chueawiang, W., Sriraksa, P., Tabmee, A., Sirinavin, S., 2022. Efficacy and safety of *Andrographis paniculata* extract in patients with mild COVID-19: a randomized controlled trial. *Arch Intern Med Res.* 5, 423-427. DOI:10.26502/aimr.0125
- Wang, G., Yang, M.L., Duan, Z.L., Liu, F.L., Jin, L., Long, C.B., Zhang, M., Tang, X.P., Xu, L., Li, Y.C., Kamau, P.M., 2021. Dalbavancin binds ACE2 to block its interaction with SARS-CoV-2 spike protein and is effective in inhibiting SARS-CoV-2 infection in animal models. *Cell Res.* 31, 17-24. <https://doi.org/10.1038/s41422-020-00450-0>
- Wiart, C., Kumar, K., Yusof, M.Y., Hamimah, H., Fauzi, Z.M., Sulaiman, M., 2005. Antiviral properties of ent-labdene diterpenes of *Andrographis paniculata* nees, inhibitors of herpes simplex virus type 1. *Phytother. Res.* 19, 1069-1070. <https://doi.org/10.1002/ptr.1765>
- Whitt, M.A., 2010. Generation of VSV pseudotypes using recombinant Δ G-VSV for studies on virus entry, identification of entry inhibitors, and immune responses to vaccines. *J. Virol. Methods.* 169, 365-74. <https://doi.org/10.1016/j.jviromet.2010.08.006>
- Xu, Z., Shi, L., Wang, Y., Zhang, J., Huang, L., Zhang, C., Liu, S., Zhao, P., Liu, H., Zhu, L. and Tai, Y., 2020. Pathological findings of COVID-19 associated with acute respiratory distress syndrome. *Lancet Respir. Med.* 8, 420-422. [https://doi.org/10.1016/S2213-2600\(20\)30076-X](https://doi.org/10.1016/S2213-2600(20)30076-X)
- Zhang, Z., Zheng, Y., Niu, Z., Zhang, B., Wang, C., Yao, X., Peng, H., Franca, D.N., Wang, Y., Zhu, Y., Su, Y., 2023. SARS-CoV-2 spike protein dictates syncytium-mediated lymphocyte elimination. *Cell Death Diff.* 28, 2765-2777. <https://doi.org/10.1038/s41418-021-00782-3>
- Zhang, Q., Tang, W., Stancanelli, E., Jung, E., Syed, Z., Pagadala, V., Saisi, L., Chen, C.Z., Gao, P., Xu, M., Pavlinov, I., Li, B., Huang, W., Chen, L., Jian, L., Xie, H., Zheng, W., Ye, Y., 2023. Host heparan sulfate promotes ACE2 super-cluster assembly and enhances SARS-CoV-2-associated syncytium formation. *Nat Commun.* 14, 5777. <https://doi.org/10.1038/s41467-023-41453-w>